

Formation of Complex XeHCl⁺ in the Xe⁺ + HCl Collision

Jongbaik Ree,* Yoo Hang Kim,[†] and Hyung Kyu Shin[‡]

Department of Chemistry Education, Chonnam National University, Gwangju 500-757, Korea. *E-mail: jbree@chonnam.ac.kr

[†]Department of Chemistry and Center for Chemical Dynamics, Inha University, Incheon 402-751, Korea

[‡]Department of Chemistry, University of Nevada, Reno, Nevada 89557, U.S.A.

Received January 23, 2008

The formation of complex XeHCl⁺ in the collision-induced reaction of Xe⁺ with HCl has been studied by use of classical dynamics procedures using the London-Eyring-Polanyi-Sato empirical potential energy surfaces. A small fraction of trajectories on the Xe⁺ + HCl and Xe + HCl⁺ surfaces lead to the formation of complex XeHCl⁺ with life-times of 1-2 ps which is long enough to survive many rotations before redissociating back to the reactant state. The formation of complex XeHCl⁺ occurs mainly from collision angle of $\Theta = 45^\circ$.

Key Words : Collision-induced complex, XeHCl⁺, Xe⁺, HCl

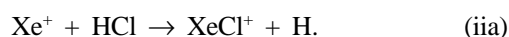
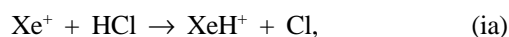
Introduction

Recent studies of ion-molecule collisions^{1,2} suggest that the dynamics of collision-induced reactions involving a heteronuclear molecule may be different from those involving a homonuclear molecule. Trajectory calculations, when based on accurate potential energy surfaces, should provide useful information for experimentalists to design and understand the dynamics of energy transfer, bond dissociation and/or bond formation in these ion-molecule collisions. The collision-induced hydrogen atom transfer step in the Xe⁺ + HCl system where the ionization potential of Xe is 12.130 eV and that of H is 13.600 eV, can lead to the production of XeH⁺.³⁻⁵ Another product which can be formed in the collision system is XeCl⁺ with a reasonably strong bond ($D_{\text{XeCl}^+} = 2.18$ eV).⁶ The protonated ion XeH⁺ has a dissociation energy (= 3.90 eV),^{4,7,8} which is not greatly different from that of HCl (= 4.4336 eV),⁹ thus Xe⁺ + HCl → XeH⁺ + Cl is nearly thermoneutral. The reaction can produce XeH⁺ and XeCl⁺, but more importantly, the Xe⁺ + HCl state can transform into the near-resonant Xe + HCl⁺ state through charge transfer, since the ionization potential of HCl, 12.748 eV,¹⁰ is very close to that of Xe. Thus, two potential energy surfaces can interact and the diatomic ions can form from both Xe⁺ + HCl and Xe + HCl⁺ states.¹¹

In a very recent paper, we have reported the formation of XeH⁺ and XeCl⁺ in the collision-induced reaction of Xe⁺ with HCl.¹¹ Because of the closeness in their ionization potentials, charge transfer Xe⁺ + HCl → Xe + HCl⁺ can readily occur, so the diatomic ions can form in the reactions



as well as in the reactions



We found that both XeH⁺ and XeCl⁺ formations occur

mainly from the perpendicular configuration, Xe⁺⋯^HCl at the turning point.

In the present paper, which is an extension to the previous work,¹¹ we report evidence of the XeHCl⁺ complex formation in the Xe⁺ + HCl collision. We present a detailed analysis of the XeHCl⁺ formation using the procedures of classical trajectory calculations.

Model and Methods

The model and theoretical procedures have been described in detail in our earlier papers,^{1,11,12} and only a brief summary is presented here. For simplicity we only outline the model for the Xe⁺ + HCl collision. In the collision geometry, the target molecule is located at the origin and the Z axis is aligned with the relative velocity vector. The Xe-H and Xe-Cl distances are $R_{\text{Xe-H, Xe-Cl}} = [R^2 + \gamma_i^2 (R_{\text{e,H-Cl}} + x)^2 \pm 2\gamma_i (R_{\text{e,H-Cl}} + x)R\cos\Theta]^{1/2}$, respectively, where $i = \text{Cl}$ with the minus sign for $R_{\text{Xe-H}}$ and $i = \text{H}$ with the plus sign for $R_{\text{Xe-Cl}}$. Here R is the distance between Xe⁺ and the center of mass (c.m.) of HCl, Θ is the angle between the Xe-to-c.m. direction and the HCl molecular axis, x is the displacement of the HCl bond from its equilibrium value $R_{\text{e,HCl}}$, and $\gamma_{\text{H,Cl}} = m_{\text{H,Cl}}/(m_{\text{H}} + m_{\text{Cl}})$. R can be related to the other collision geometry parameters as $R = (\rho^2 + z^2)^{1/2}$, where ρ measures the position of Xe⁺ from the Z axis, its initial ($t = t_0$) value being the impact parameter b , and z is the vertical distance from Xe⁺ to the XY plane. The orientation angle Θ can then be related to the collision coordinates, θ , ϕ , R and ρ as

$$\cos\Theta = [(R^2 - \rho^2)^{1/2}\cos\theta + \rho\sin\theta\cos(\phi - \phi')]/R, \quad (1)$$

where θ measures the rotation of HCl from the Z axis and ϕ is its azimuthal, whereas ϕ' measures the projection of Xe⁺ on the XY plane.¹ Thus, the coordinates (x, θ, ϕ) describes the motion of HCl, while (z, ρ, ϕ') describes the motion of Xe⁺ toward HCl. Here the azimuthal angle ϕ' may be eliminated by rotating the coordinate system about the Z axis.

We use the London-Eyring-Polanyi-Sato (LEPS) proce-

ture¹³⁻¹⁵ to construct the potential energy surface (PES) as a function of the three distances $R_{\text{H-Cl}}$, $R_{\text{Xe-H}}$ and $R_{\text{Xe-Cl}}$. The coulombic and exchange terms in the procedure are, respectively,

$$Q_i = 1/4 D_i (1 + \Delta_i)^{-1} \times [(3 + \Delta_i) e^{(R_{e,i} - R_i)/a_i} - (2 + 6\Delta_i) e^{(R_{e,i} - R_i)/2a_i}], \quad (2a)$$

$$A_i = 1/4 D_i (1 + \Delta_i)^{-1} \times [(1 + 3\Delta_i) e^{(R_{e,i} - R_i)/a_i} - (6 + 2\Delta_i) e^{(R_{e,i} - R_i)/2a_i}], \quad (2b)$$

for $i = \text{HCl}$, XeH^+ and XeCl^+ , where Δ_i is the adjustable Sato parameter. Here D_i is related to the dissociation energy, $D_{0,i}^0$ as $D_i = D_{0,i}^0 + 1/2 \hbar \omega_i$, where $\omega_i = 2\pi c \omega_{e,i}$ and $\omega_{e,i}$ is the fundamental frequency in cm^{-1} . The parameters D_i , equilibrium atom-atom distance $R_{e,i}$ and exponential range parameter a_i needed to construct potential energy surfaces in the reaction region are listed in Ref. 11.

When the collision partners approach each other from a large distance, the incoming collision trajectory is determined by the interaction of Xe^+ with the center of mass of HCl , which can be described by an exponential function, such as the Morse-type potential energy or an inverse-power function such as the Lennard-Jones (LJ) type for the neutral part, along with the induction energy. For the neutral part, we take the Morse function: $U_{\text{neu}}(R) = D[e^{(R_e - R)/a} - e^{(R_e - R)/2a}]$, where the potential parameter $D = 0.0236$ eV at $R_e = 4.16$ Å,¹⁶ and the exponential range parameter $a = 0.275$ Å.¹¹ In addition to the charge-permanent dipole interaction $U_{c,\mu} = -e\mu_{\text{HCl}}\cos\Theta/(4\pi\epsilon_0)R^2$, Xe^+ induces in HCl a dipole moment, which produces the charge-induced dipole interaction $U_{c,\text{ind}\mu} = e^2\alpha_{\text{HCl}}/2(4\pi\epsilon_0)R^4$ where $\mu_{\text{HCl}} = 1.084$ debye and $\alpha_{\text{HCl}} = 2.63$ Å³.¹⁶ Because $U_{c,\mu}$ is replaced by zero if HCl undergoes rapid rotation, the induction effect is largely determined by the orientation independent term $U_{c,\text{ind}\mu}$, which is 6.31×10^{-2} eV at $R = R_e$. Similarly, for $\text{Xe} + \text{HCl}^+$, $U_{c,\text{ind}\mu} = 9.69 \times 10^{-2}$ eV. A strong attractive interaction coming from the induced dipole moment will affect the interaction between the collision partners during the approach. That is, the effects of the induction energy are important in ion-molecule interactions since the energy speeds up the approaching collision partners so the kinetic energy of the relative motion is increased and modifies the slope of the repulsive part of the reaction-zone interaction potential on which the efficiency of the bond dissociation depends sensitively.^{1,2}

Results and Discussion

The best set of the Sato parameters are found to be $\Delta_{\text{H-Cl}} = 0.104$, $\Delta_{\text{Xe}^+ - \text{H}} = -0.552$ and $\Delta_{\text{Xe}^+ - \text{Cl}} = 0.712$.¹¹ The LEPS potential function has the functional dependence of $U(R, x, \theta, \phi, \rho)$, where R is a more general collision coordinate than z . The Hamiltonian H is then the sum of this function and kinetic energy terms $p_j^2/2m_j$ for $j = R, x$ and $p_j^2/2I$ for $j = \theta, \phi$, where m_x and I are the reduced mass and moment of inertia of HCl , respectively. Thus we can study the dynamics of

molecular collisions by solving the Hamilton's equations. The computational procedure employed in the present study including the expressions determining the initial conditions at $t = t_0$ obtained for the intermolecular and intramolecular motions is the same as those used in previous studies.^{1,2} The initial conditions of vibrational and rotational energies ($E_{v,\text{HCl}}^0$, $E_{r,\text{HCl}}^0$) with corresponding phases, impact parameter b , which is the initial value of ρ , and rotational angles $\theta(t_0)$ and $\phi(t_0)$ are sampled randomly.

The presence of strong attraction between the reactants and the XeCl^+ formation through the indirect-mode mechanism suggest the possibility of the collision partners forming a long-lived complex XeHCl^+ , where the light H atom oscillates back and forth between the two massive atoms. That is, the complex can survive for a time scale longer than its rotational period. The formation of such a complex surviving for a time comparable to the rotational period of the complex in $\text{Ar}^+ + \text{D}_2 \rightarrow \text{ArD}^+ + \text{D}$ and $\text{N}_2^+ + \text{D}_2 \rightarrow \text{N}_2\text{D}^+ + \text{D}$ at the lower end of the energy range of 6 - 100 eV has been reported by Doverspike *et al.*¹⁷ On the other hand, in $\text{Ar}^+ + \text{H}_2/\text{D}_2$ at the lower energy region of 2-30 eV, Fink and King reported that their measurements of the broadening and the product peak of $\text{ArH}^+/\text{ArD}^+$ cannot be attributed to complex formation.¹⁸ As Θ increases toward the right angle, the skewness of the PES relaxes and the saddle

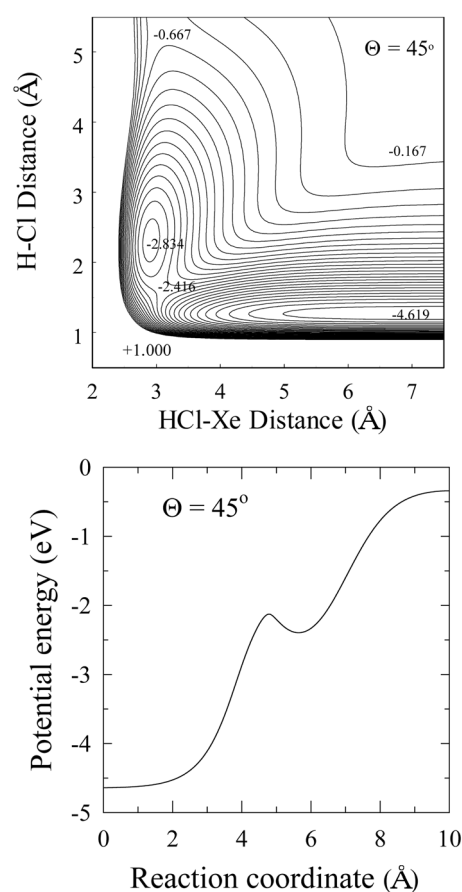


Figure 1. Potential energy surface for $\Theta = 45^\circ$ and $b = 0$. The labeled contours are in eV. The bottom frame shows variation in the minimum energy path.

point landscape changes. For an intermediate angle of $\Theta = 45^\circ$ and $b = 0$, the PES shows a shallow basin of the depth 0.283 eV immediately beyond the barrier; see Figure 1. The collision system can now be trapped in the basin, forming a weakly bound complex XeHCl^+ . The profile of minimum energy path also shown in Figure 1 is particularly interesting, because it shows a shallow basin significantly high up from the entrance valley floor “hanging” on the side of the potential energy wall, which blocks the trajectory traveling toward the exit valley. That is, the trajectory returns to the entrance valley after a long residency in the basin, which is much longer than the vibrational period of HCl^+ , or it can even reach the plateau region of $\text{H} + \text{Cl}$. Although it is deeper, the presence of such a basin has been predicted in $\text{Ar}^+ + \text{H}_2$ by Kuntz and Roach.¹⁹

We find that the number of trajectories trapped in a basin is not large. For example, at $E = 7$ eV, out of 40000 trajectories sampled 766 trajectories are trapped in the basin on the $\text{Xe}^+ + \text{HCl}$, whereas 505 trajectories are trapped on the $\text{Xe} + \text{HCl}^+$ surface. At the energy as high as 20 eV, the numbers of trapped trajectories are much smaller; on the corresponding PESs they are only 38 and 20, respectively. The probability of XeHCl^+ formation defined as the ratio of the total number of trapped trajectories to 40 000 sampled is plotted in Figure 2 as a function of the collision energy, the total number being the sum of two contributions divided by 2. The probability closely follows a Gaussian distribution, showing a maximum value of 0.016 at an intermediate energy of 7 eV.

We choose a representative trajectory for the XeHCl^+ formation at $E = 6$ eV, where 397 trajectories are trapped, and plot its time evolution in Figure 3. The complex of this representative case survives for 1.2 ps, which is the period between the initial turning point and the instance when the H-Cl and Xe-H distances diverge. During the period, both distances undergo a large amplitude oscillation with nearly identical frequencies. Furthermore, the H-Cl and Xe-Cl distances are large and H-Cl oscillates around Xe-Cl, whereas the Xe-H distance is short and oscillates near its equilibrium value 1.603 Å. The time evolution of these distances and their magnitudes clearly indicate the configuration of the

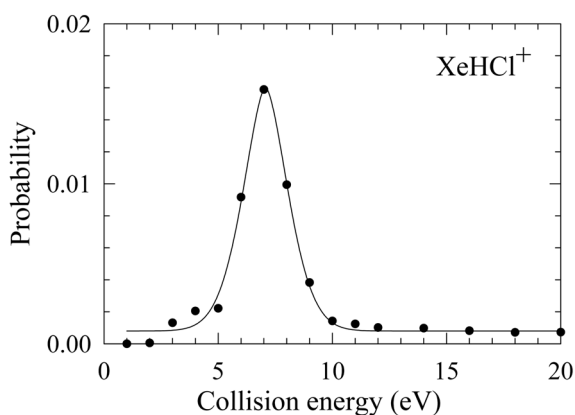


Figure 2. Dependence of the probability of XeHCl^+ formation on the collision energy.

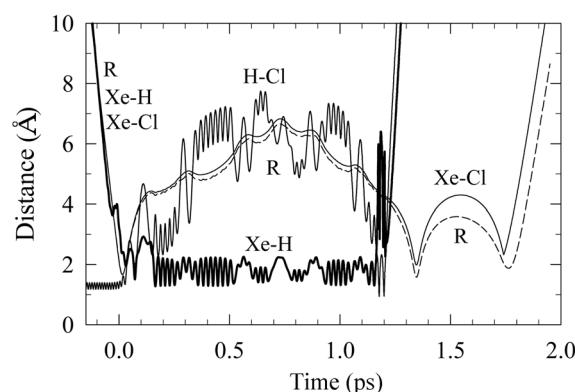


Figure 3. Time evolution of atom-atom distances in the complex XeHCl^+ for a representative trajectory at $E = 6$ eV. The distances R, Xe-H and Xe-Cl in the incoming region are indistinguishable. The outgoing H-Cl and Xe-H distances are very close to each other.

complex is triangular with an acute $\angle \text{HCIXe}$ angle, and H undergoes rapid vibration relative to the two heavy atoms in the complex. It is particularly interesting to note in Figure 3 that the Xe-Cl distance finally diverges at $t = +1.8$ ps, *i.e.*, the Xe-Cl bond survives for an additional period of 0.6 ps after the Xe-H dissociation, because the lighter H atom can escape more easily from the XeHCl^+ complex. For many trapped trajectories sampled, the complex survives for 1–2 ps, which far exceeds 0.4–0.6 ps, the time scale of the XeCl^+ formation through the indirect-mode mechanism.¹¹

To compare the time scale for the lifetime of XeHCl^+ noted in Figure 3 with the rotational period, we first consider the collinear configuration. The moment of inertia for the linear complex Xe-H-Cl^+ at the equilibrium is $I_{\text{XeHCl}^+} = 3.90 \times 10^{-45} \text{ kg m}^2$, which gives the rotational energy $8.90 \times 10^{-6} J_{\text{XeHCl}^+} (J_{\text{XeHCl}^+} + 1) \text{ eV}$. At 300 K, the temperature at which the internal states of the target molecule are sampled, the most populated rotational state is $J_{\text{XeHCl}^+, \text{max}} = 37$ and its rotational period is 0.313 ps. For the perpendicular configuration, again assuming the equilibrium bond distances, we find $I_A = 2.58 \times 10^{-45} \text{ kg m}^2$, $I_B = 2.59 \times 10^{-45} \text{ kg m}^2$ and $I_C = 1.14 \times 10^{-47} \text{ kg m}^2$ *i.e.*, $I_A \approx I_B \gg I_C$, with which the complex being approximated as a symmetric rotor. The rotational energy expression can then be written as $E_{JK} = 1.35 \times 10^{-5} J_{\text{XeHCl}^+} (J_{\text{XeHCl}^+} + 1) + 3.4 \times 10^{-3} K_{\text{XeHCl}^+}^2$ in eV, where $K_{\text{XeHCl}^+} = 0, \pm 1, \pm 2, \dots, \pm J_{\text{XeHCl}^+}$ and the energy level is $2(2 J_{\text{XeHCl}^+} + 1)$ -fold degenerate except for $K = 0$. We can consider two limiting cases. When $K_{\text{XeHCl}^+} = 0$, the complex has no angular momentum about its principal axis and it undergoes end-over-end rotation and the rotational period is 0.207 ps. On the other hand, when $J_{\text{XeHCl}^+} \approx |K_{\text{XeHCl}^+}|$, the angular momentum arises from rotation around the principal axis and the rotational period is almost 1 fs, which is physically not plausible in the present system. In the complex state in which the light H atom protruding from the direction of two heavy atoms, we believe the relation $|K_{\text{XeHCl}^+}| \ll J_{\text{XeHCl}^+}$ will hold. Therefore, although the rotational energies calculated are only a rough estimate and the configurations are not strictly linear or perpendicular, the numbers calculated above clearly show that the complex

with a lifetime of 1-2 ps can undergo at least several rotations during its residency in the basin, the time scale being much longer than that noted in ArD_2^+ , N_2D_2^+ and ArH_2^+ .^{17,18}

Concluding Comments

The present paper reports the result of trajectory calculations of the formation of the complex XeHCl^+ in the collision-induced $\text{Xe}^+ + \text{HCl}$ reaction over the collision energy range of 2-20 eV. The collision complex XeHCl^+ is found to be significant, especially at lower collision energies. The collision configuration intermediate between the

linear $\text{Xe}^+ \cdots \text{H}-\text{Cl}$ and perpendicular $\text{Xe}^+ \cdots \overset{\text{H}}{\text{Cl}}$ configurations favors the formation of the complex. The lifetimes of complexes lie between 1 and 2 ps, which greatly exceed the rotational period of the complex.

Acknowledgements. YHK gratefully acknowledges the financial support from Inha University. Computational time was supported by the Eighth Supercomputing Application Support Program from the Korea Institute of Science and Technology Information (KISTI) and the University of Nevada Reno Chemistry Computational Program.

References

1. Akin, F. A.; Ree, J.; Ervin, K. M.; Shin, H. K. *J. Chem. Phys.* **2005**, *123*, 064308.
2. Ree, J.; Kim, Y. H.; Shin, H. K. *J. Chem. Phys.* **2006**, *124*, 074307.
3. Moore, C. E. *Ionization Potentials and Ionization Limits Derived from the Analysis of Optical Spectra*; Natl. Stand. Ref. Data Ser., Natl. Bur. Stand. 34: U. S. GPO, Washington, DC., 1970.
4. Rogers, S. A.; Brazier, C. R.; Bernath, P. F. *J. Chem. Phys.* **1987**, *87*, 159.
5. *CRC Handbook of Physics and Chemistry*, 64th ed.; Weast, R. C., Ed.; CRC Press: Boca Raton, FL, 1983; p. E-61 and E-63.
6. Schröder, D.; Harvey, J. N.; Aschi, M.; Schwarz, H. *J. Chem. Phys.* **1998**, *108*, 8446.
7. Klein, R.; Rosmus, P. *Z. Naturforsch. Teil A* **1984**, *39*, 349.
8. Peterson, K. A.; Petrmichl, R. H.; McClain, R. L.; Woods, R. C. *J. Chem. Phys.* **1991**, *95*, 2352.
9. Huber, K. P.; Herzberg, G. *Constants of Diatomic Molecules*; Van Nostrand Reinhold: New York, 1979; p 240 and 284.
10. Tonkyn, R. G.; Wiedmann, R. T.; White, M. G. *J. Chem. Phys.* **1992**, *96*, 3696.
11. Ree, J.; Kim, Y. H.; Shin, H. K. *J. Chem. Phys.* **2007**, *127*, 054304.
12. Lee, S.; Ree, J.; Kim, Y. H.; Shin, H. K. *Bull. Korean Chem. Soc.* **2005**, *26*, 1369.
13. Glasstone, S.; Laidler, K. J.; Eyring, H. *The Theory of Rate Processes*; McGraw-Hill: New York, 1941.
14. Sato, S. *J. Chem. Phys.* **1955**, *23*, 592, 2465.
15. Ree, J.; Kim, Y. H.; Shin, H. K. *Bull. Korean Chem. Soc.* **2007**, *28*, 635.
16. Hirschfelder, J. O.; Curtiss, C. F.; Bird, R. B. *Molecular Theory of Gases and Liquids*; John Wiley: New York, 1967; p 27 for $U_{c,ind \mu}$ and $U_{c,\mu}$ p. 950 for α_{HCl} , p. 1110 and 1200 for ϵ and σ .
17. Doverspike, L. D.; Champion, R. L.; Bailey, T. L. *J. Chem. Phys.* **1966**, *45*, 4385.
18. Fink, R. D.; King, J. S. Jr. *J. Chem. Phys.* **1967**, *47*, 1857.
19. Kuntz, P. J.; Roach, A. C. *J. Chem. Soc., Faraday Trans. II* **1972**, *68*, 259.